Available online at www.sciencedirect.com

ScienceDirect

Procedia Structural Integrity 57 (2024) 161–168

Structural Integrity Procedia

www.elsevier.com/locate/procedia

Fatigue Design 2023 (FatDes 2023)

Fatigue behaviour of 25% wt. short glass fibre reinforced recycled Polypropylene filled with mineral filler in presence of notches

Andrea Resente[a], Mauro Ricotta[a,*], Marco Garilli[b] and Giovanni Meneghetti[a]

[a]*Department of Industrial Engineering, University of Padova, Via Venezia 1, 35131 Padova, Italy*
[b]*Electrolux Appliances SPA, Via Lino Zanussi 24, 33080 Porcia, Italy*

Abstract

An experimental investigation is presented regarding the fatigue behaviour of notched and plain specimens made of 25% wt. short glass fibre reinforced recycled Polypropylene filled with mineral filler. Plain and double-edge notched specimens (with notch radius ranging from 0.2 mm to 10 mm) were produced by injection moulding and tested under tension-compression fatigue to highlight the effect of the notch root radius and notch geometry. During the fatigue tests, the damage evolution was monitored using a traveling microscope to define the number of cycles spent for the fatigue crack nucleation. First, the fatigue tests were reanalysed in terms of net-stress amplitude and the traditional stress-life curves for each specimen's geometry were found. Then, an energy-based approach was proposed for the assessment of fatigue life spent for the crack nucleation. The model is conceptually based on the actual damage evolution observed during the fatigue tests, which was according to the technical literature: the initiation of a macro crack results from the accumulation of damage in the matrix. Thus, the strain energy density evaluated in the matrix and averaged on a structural volume embracing the notch tip was adopted as fatigue damage index to correlate in a single scatter band the fatigue data of plain and notched specimens.

* Corresponding author. Tel. 049-827-6762 ; fax: 049-827-6785 .
E-mail address: mauro.ricotta@unipd.it

1. Introduction

The injection moulding process is widely used in the industrial production of components in polymeric materials, due to its high production rates. When the material is reinforced with short fibers, their distribution determines the local mechanical properties of the component and it is influenced by process parameters and primarily the gates

10.1016/j.prostr.2024.03.019

locations, as indicated by Bernasconi et al. (2015), but also the melt temperature, volumetric flow and cooling circuits' temperature as reported by many authors, such as De Monte et al. (2010), Pietrogrande et al. (2021), Ricotta et al. (2021) and Ivan et al. (2022).

Different criteria have been proposed to estimate the static strength, as reported by Whitney et al. (1974), Toll et al., (1992) and Ibáñez-Gutiérrez et al. (2016), and the fatigue life, as done by Castagnet et al. (2021), of components, taking into account the fiber distribution, which can be estimated using injection moulding simulations or, in some cases, as done by Pietrogrande et al. (2019), observed using μCT analysis. Geometrical notch effects highly influence the fatigue life of components because of the well-known stress concentration phenomenon, as reported by Bernasconi et al. (2015), Belmonte et al. (2016) and Mortazavian and Fatemi (2016). Finally, the presence of a certain fraction of recycled polymeric matrix is another factor that influences the mechanical properties and causes a decrease in both the strength and the stiffness, as reported in Meneghetti et al. (2015) and Rigon et al. (2021).

Nomenclature

E	Young Modulus
IM	Injection Moulding
K_{tn}	Linear elastic stress concentration factor referred to the net-section
R_c	Control Radius for the SED and the SEDm criterion in case of cracks or sharp notches
SED	Strain Energy Density
SEDm	Strain Energy Density on the matrix constituent
w_n	Width of the net-section of the specimen
σ_{nf}	Tensile net-stress at Failure

2. Material, specimens and test methods

The material analysed in this study is a polypropylene matrix (47% virgin polypropylene and 53% post-consumer recycled polypropylene) reinforced by 25% wt. of short glass fibre and filled with 21% wt. of calcium carbonate and 1% wt. of maleic anhydride as coupling agent between the fibres and the matrix.

To highlight the notch effect, net-shape notched specimens and plaques according to the geometries reported in Figure 1 have been produced by injection moulding (IM), using a Zhafir Zeres 1900 press, with the process conditions reported in Table 1. The plain specimens have been milled from the plaques as reported in Figure 1.

Table 1. IM conditions used for the production of the specimens.

Specimen	$T_{melt\ flow}$ [°C]	$T_{cooling\ circuits}$ [°C]	$P_{packing}$ [MPa]	$t_{packing}$ [s]	Volumetric Flow [cm^3/s]
Plaque 200x75	220	50	40	12	159
Notched specimens	225	30	40	12	143
Plaque 200x32	225	30	40	12	143

Displacement controlled tensile tests on milled plain specimens were carried out imposing a displacement rate equal to 2 mm/min, using a StepLab EA05 electric machine equipped with a 5 kN-load cell and a MTS Model 632.13F-20 extensometer with a gauge length of 10mm. The static tests on net-shape notched specimens have been executed using a 15 kN-load cell MTS 858 Mini Bionix II servo-hydraulic machine and the strain rate was measured using a MTS Model 634.12F-24 extensometer with a gauge length of 25mm with the knives straddling the notched section. The imposed displacement rate was such that the average strain rate evaluated in the net-section was approximatively equal to that applied to the milled plain specimens. Load-controlled, tension-compression (load ratio, R=-1) fatigue tests were carried out using the StepLab EA05 machine, by imposing load test frequency ranging from 4 to 10 Hz, depending on the applied stress amplitude, to ensure that the temperature of the specimens was always between 23°C

and 26°C. In more detail, the material temperature was monitored using a thermocouple, fixed close to the notch tip or in the middle of the net-section in the case of notched or plain specimens, respectively.

During the static and fatigue tests, the damage evolution was monitored taking advantage of DinoLite digital microscopes, operating with a magnification ranging from 20x to 220x. In detail, the fatigue life spent for crack nucleation, N_i, was defined as the number of cycles when the first crack (with an approximate size of 0.1mm) emanating from one of the notch tips was detected on the specimen's surfaces. In the case of milled plain specimens, the crack nucleation (which occurs at the base of the fillet) was followed by the failure of the specimens within few cycles, therefore it has been considered N_i=N_f, where N_f indicates the number of cycles at failure of the specimens.

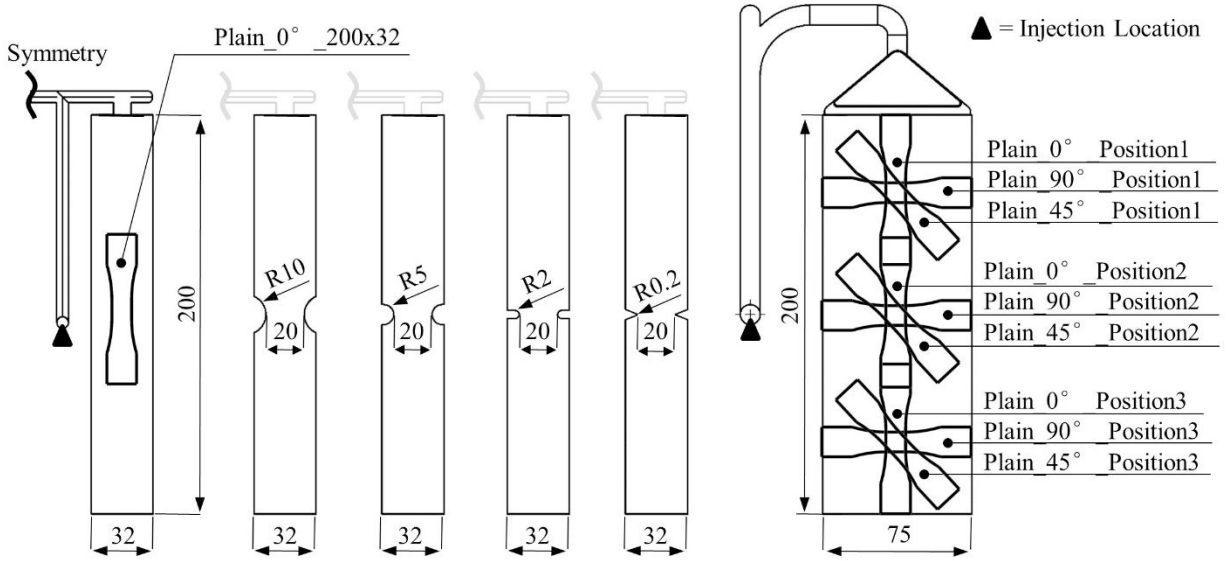

Figure 1. Geometry of the specimens. Measurements in millimeters. Specimens' thickness is reported in Table 2.

3. Quasi-static tensile test results

The results of quasi-static tensile tests are summarized in Table 2, where the average values are reported along with an indicator of the experimental scatter, $\Delta_{\%}$, which was calculated as:

$$\Delta_{\%} = \frac{max(y_i) - min(y_i)}{2\ average(y_i)} \cdot 100 \quad \text{,where y = E, } \sigma_{nf} \tag{1}$$

Regarding the milled plain specimens, the highest elastic modulus and static strength were found for Plain_0°_200x32 specimens, while the lowest for Plain_45°_Position3. Moreover, Table 2 shows that for a given orientation angle θ (i.e. the angle between the tensile load and the nominal flow direction) and in light of the observed experimental scatter, there is a negligible influence of the position from which the specimens were machined.
Concerning notch sensitivity, Table 2 highlights that σ_{nf} decreases when the notch radius is reduced from 10 to 2 mm, while the notch effect disappears if the notch radius is reduced further from 2 to 0.2 mm.

It is worth of noting that σ_{nf} of the R10 and R5 specimens is higher than the static strength of all plain specimens. This difference was observed by Toll and Aronsson (1992) referring to milled and net-shape specimens and it is due to the fibre distribution. Fibres, indeed, tend to be strongly aligned in the flow direction near the mould surfaces as compared to the inner portion of the specimens. Therefore, these regions have a higher local strength against a tensile load applied along the flow direction. Due to the milling operations performed to obtain the plain specimens, these stronger regions of material are removed, as sketched in Figure 2, causing a decrease of the static strength of milled plain specimens compared to the net-shape notched specimens. Another factor that could contribute to increasing the strength of the notched specimens is the hourglass shape of the specimens: during the IM process, this shape causes a

local increase of the velocity of the melt flow in the net-section, which makes the fibers reorient along the flow direction, as indicated by Folgar and Tucker (1984) and then strengthen the net-shape notched specimens.

Table 2. Experimental results of the quasi-static tensile tests.

Specimen	E [MPa]	σ_{nf} [MPa]	Thickness [mm]	w_n [mm]	$n_{specimens}$	K_{tn}
Plain_0°_Position1	6124 ± 2%	49 ± 1%	1.6	10	3	/
Plain_0°_Position2	6100 ± 3%	49 ± 1%	1.6	10	3	/
Plain_0°_Position3	6229 ± 1%	49 ± 0%	1.6	10	3	/
Plain_0°_200x32	6166 ± 6%	52 ± 0%	4.8	10	3	/
Plain_45°_Position1	4953 ± 6%	39 ±1%	1.6	10	3	/
Plain_45°_Position2	4629 ± 7%	37 ± 1%	1.6	10	3	/
Plain_45°_Position3	4178 ± 3%	34 ± 5%	1.6	10	3	/
Plain_90°_Position1	5388 ± 2%	38 ± 1%	1.6	10	3	/
Plain_90°_Position2	5565 ± 6%	36 ± 1%	1.6	10	3	/
Plain_90°_Position3	5274 ± 6%	36 ± 2%	1.6	10	3	/
R10	/	58 ± 3%	4.8	19.2	3	1.72
R5	/	54 ± 2%	4.8	19.2	3	2.16
R2	/	51 ± 2%	4.8	19.2	3	3.10
R02	/	51 ± 2%	4.8	19.2	3	7.96

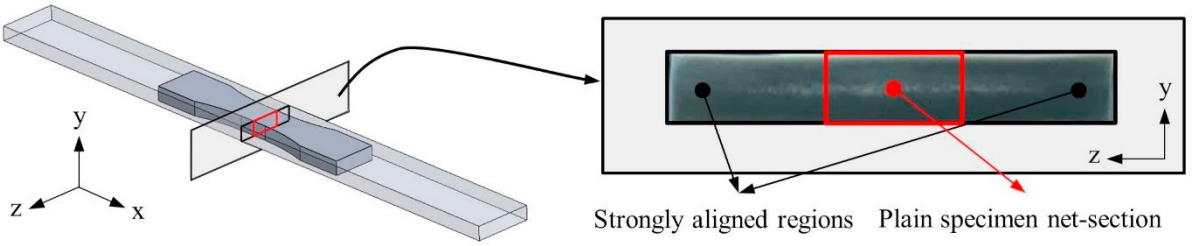

Figure 2. Image of the net-section 200x32mm plaque.

4. Fatigue test results

Tension-compression axial fatigue tests have been executed on milled Plain_0°_200x32 specimens and net-shape notched specimens with notch radius of 0.2mm, 2mm and 10mm. Results are reported in Figure 3 in terms of net-stress amplitude $\sigma_{n,a}$, along with the fatigue curves obtained using to Eq.(2) and the relative stress-based scatter index, T_σ (calculated as the stress ratio between the 5% and 95% survival probability curves, with a confidence index of 95%).

$$\sigma_{n,a}^{k} \cdot N_i = cost \tag{2a}$$

$$\sigma_{n,a}^{k} \cdot N_f = cost \tag{2b}$$

A total of 32 specimens have been tested: 4 plain specimens, 10 R02 specimens, 4 R2 specimens and 4 R2 specimens.

It is worth noting that the fatigue strength of milled plain specimens is lower than that relevant to the net-shape R10 specimens, as observed during the quasi-static tensile tests. Figure 3 also shows that a moderate notch effect was

observed: the ratio between the reference fatigue strength at 2 million cycles, $\sigma_{n,A,}$, relevant to the most blunt notch (R10) and the most severe notch (R02) is 23.6/18.7=1.26, which is lower than $K_{tn,R02}/K_{tn,R10}$=4.63 (see Table 2). Finally, by comparing Figure 3a) to Figure 3b) it is possible to state that the crack initiation N_i for the most severely notched specimens usually occurred at a relative number of cycles (N_i/N_f) lower than for the more blunt-notched specimens: the value of N_i/N_f ranged from 0.85 to 0.99 for the R10 specimens, from 0.71 to 0.72 for the R2 specimens and from 0.49 to 0.81 for the R02 specimens and, for a given notch geometry, the highest values were observed for the largest applied stress amplitude.

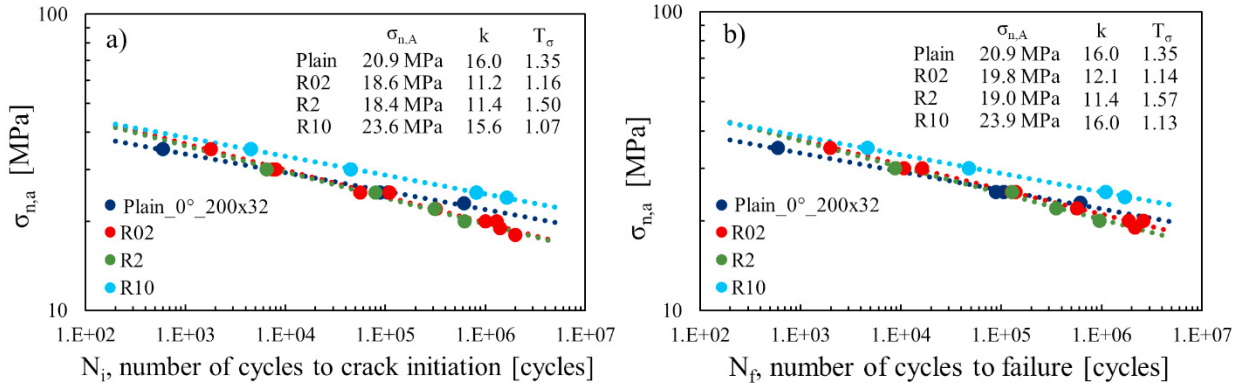

Figure 3. Result of fatigue tests for a) crack initiation and b) fatigue failure.

5. Fatigue life assessment using Matrix Strain Energy Density (SEDm) Criterion

A widely used failure criterion for notch fatigue is the Strain Energy Density (SED) Criterion. This model is based on the concepts developed by Sih (1974) and was originally proposed by Lazzarin and Zambardi (2001) for isotropic materials. Later on, the model has been adopted for short- and long-fibre reinforced composites by De Monte et al. (2007), Ibáñez-Gutiérrez et al, (2018) and Sanchez et al. (2021). Under mode I loading, the SED criterion assumes that a crack initiates when the elastic strain energy density SED averaged in a small cylindrical volume having radius R_c embracing a crack or a sharp notch reaches a critical value W_c. For blunt notches, a crescent shape volume must be considered with its centre located at a distance equal to r_0, calculated using Eq. (3), from the apex of the notch and a radius equal to r_0+R_c, as sketched in Figure 4.

$$r_0 = R\,\frac{\pi-2\alpha}{2\pi-2\alpha} \tag{3}$$

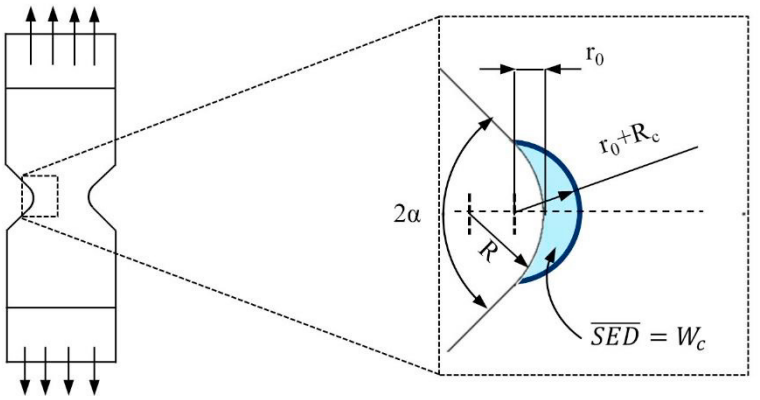

Figure 4. SED criterion for blunt-notched specimens.

Both W_c and R_c depend on the material. Considering that the actual fatigue damage of Short Fibre Reinforced Composites nucleates and propagates in the polymeric matrix, as observed by Bernasconi et al. (2007) and Belmonte et al. (2016), a modified SED approach is proposed and referred as SEDm criterion. In this criterion, the fatigue life of the component is correlated to the range of the strain energy density of the matrix constituent, ΔW_m, averaged in the structural volume, where the size of the structural volume R_c is calculated by equating the characteristic value $\Delta\overline{W_{m,c}}$ of a blunt and a severe notch at 2 million cycles. In view of this, first the fibre distribution must be evaluated using IM finite element simulations, then a structural analysis must be performed to calculate the stress and strain fields, taking into account the fibre orientation. Then the Multi-Continuum Theory, MCT, as done by Hansen and Garnich (1995), was adopted to calculate the matrix strain energy density for each structural finite element, which was finally averaged in the structural volume. In this work, Moldflow 2019 has been used for IM simulations, Ansys 2019-R1 for structural analysis, Helius 2019 for the application of the MCT and Matlab 2022a to average W_m in the structural volume. According to the results available in this investigation, the R_c value was evaluated equal to 4.3 mm.

Figure 5a and 5b show the crack initiation fatigue data reanalysed as an unique statistic population in terms of net-stress amplitude $\sigma_{n,a}$, according to Eq. (2a), along with the relative scatter band for a survival probability of 5%-95% and a confidence level of 95%. The same data have been reanalysed in terms of range of strain energy density on the matrix averaged in the structural volume, $\Delta\overline{W_m}$, according to Eq. (4):

$$\Delta\overline{W_m}^{k} \cdot N_i = cost \tag{4}$$

and are reported in Figure 5b, along with the relative scatter band for a survival probability of 5%-95% and a confidence level of 95%.

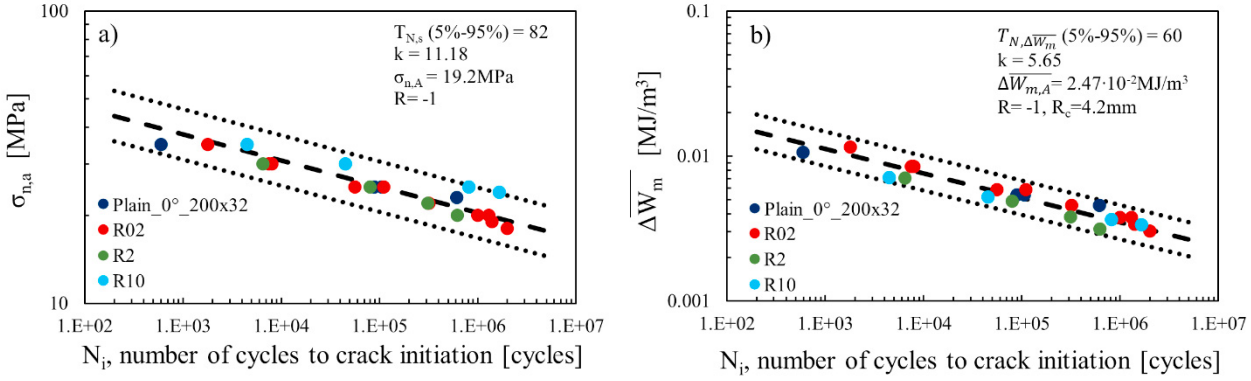

Figure 5. Fatigue life curves, expressed in a) $\sigma_{n,a}$ and b) $\Delta\overline{W_m}$ - Number of cycles at crack initiation.

According to Figure 5, the proposed criterion successfully rationalises the fatigue data with the life-based scatter index $T_{N,\Delta\overline{W_m}}$ = 60 (calculated as the life ratio between the 5% and 95% survival probability curves) and lower than $T_{N,\sigma}$= 82 relevant to the stress-life curve (Figure 5a).

6. Conclusions

In this paper, the static and fatigue behaviour of 25% wt. short glass fibre reinforced recycled Polypropylene filled with mineral filler have been investigated, highlighting the notch effect. To this end, milled plain and net-shape notched specimens (notch radius ranging from 0.2mm to 10mm) were produced by injection moulding. Based on the obtained results, the following conclusions can be drawn:

- the static strength and the reference fatigue strength of the milled plain specimens were lower than the values relevant to the net-shape notched specimens with the highest notch radius (R=10 mm), because of the different fibre distributions between milled and net-shape specimens.
- under quasi-static tensile load, a reduced notch sensitivity was found: the ratio between the static strength, $\sigma_{nf,}$, relevant to the most blunt notch (R10) and the most severe notch (R02) is 58/51=1.14, which is lower than $K_{tn,R02}/K_{tn,R10}$=4.63.
- under fully reversed axial fatigue loading, the notch effect is comparable to the quasi-static case: in fact, the ratio between the reference fatigue strength at 2 million cycles, $\sigma_{n,A,}$, relevant to the most blunt notch (R10) and the most severe notch (R02) is 23.6/18.7=1.26, which is lower than $K_{tn,R02}/K_{tn,R10}$=4.63.
- an energy-based criterion for fatigue crack initiation has been applied to correlate the fatigue data in a single design scatter band with a fatigue life-based scatter index $T_{N,\Delta\overline{W_m}} = 60$, which resulted lower than $T_{N,\sigma}$= 82 referred to the stress-based life fatigue curve.

Acknowledgements

The authors would like to express their gratitude for the doctoral fellowship program PON "Ricerca e Innovazione" 2014-2020, Action IV.5 "Dottorati su tematiche Green." 2 - DM 1061/202.

References

Bernasconi, A., Conrado, E., Hine, P., 2015. An experimental investigation of the combined influence of notch size and fibre orientation on the fatigue strength of a short glass fibre reinforced polyamide 6. Polymer testing 47: 12-21.

De Monte, M., Moosbrugger, E., Quaresimin, M., 2010. Influence of temperature and thickness on the off axis behaviour of short glass fibre reinforced polyamide 6.6 – Quasi-static loading. Composites Part A: Applied Science and Manufacturing 41, 859–871.

Pietrogrande, R., Carraro, P., De Monte, M., Quaresimin, M., 2021. Modelling the influence of the microstructure on the high cycle fatigue crack initiation in short fibre reinforced thermoplastics. Composites Science and Technology 201.

Ricotta, M., Sorgato, M., Zappalorto, R., 2021. Tensile and compressive quasi-static behaviour of 40% short glass fibre - PPS reinforced composites with and without geometrical variations. Theoretical and Applied Fracture Mechanics 114.

Ivan, R., Sorgato, M., Zanini, F., Lucchetta, G., 2022. Improving Numerical Modeling Accuracy for Fiber Orientation and Mechanical Properties of Injection Molded Glass Fiber Reinforced Thermoplastics. Materials 15(13): 4720.

Whitney, J.M., Nuismer, R.J., 1974. Stress fracture criteria for laminated composites containing stress concentrations. Journal of Composites Materials 8(2): 253-65.

Toll, S., Aronsson, C.G., 1992. Notched strength of long- and short- fibre reinforced polyamide. Composites Science and Technology 45.

Ibáñez-Gutiérrez, F.T., Cicero, S., Carrascal, I.A., Procopio, I., 2016. Effect of fibre content and notch radius in the fracture behaviour of short glass fibre reinforced polyamide 6: An approach from the Theory of Critical Distances. Composites part B: Engineering 94: 299-311.

Castagnet, S., Nadot-Martin, C., Fouchier, N., Conrado, E., Bernasconi, A., 2021. Fatigue life assessment in notched injection-molded specimens of a short-glass fiber reinforced Polyamide 6 with different injection gate locations. International Journal of Fatigue 143: 105968.

Pietrogrande, R., Carraro, P.A, De Monte, M., Quaresimin, M., 2018. A novel pseudo-grain approach for the estimation of elastic stress distributions within the matrix of short fiber-reinforced polymers. Composites part B 150: 115-123.

Belmonte, E., De Monte, M., Riedel, T., Quaresimin, M., 2016. Local microstructure and stress distributions at the crack initiation site in a short fiber reinforced polyamide under fatigue loading. Polymer testing 54: 250-259

Mortazavian, S., Fatemi, A., 2016. Effects of mean stress and stress concentration on fatigue behavior of short fiber reinforced polymer composites. Fatigue & Fracture of Engineering Materials & Structures 39: 149-166.

Meneghetti, G., Ricotta, M., Sanità, M., Refosco, D., Atzori, B., 2015. Notch sensitivity of fully reversed axial fatigue behaviour of different polypropylene compounds. Procedia Engineering 109: 441-449.

Rigon, D., Ricotta, M., Ardengo, G., Meneghetti, G., 2021. Static mechanical properties of virgin and recycled short glass fiber-reinforced polypropylene produced by pellet additive manufacturing. Fatigue and Fracture of engineering materials & Structures 44(9): 25 54–2569.

Folgar, F., Tucker, C.L., 1984. Orientation Behaviour of Fibers in Concentrated Suspensions. Journal o Reinforced Plastics and Composites 3 (2): 98-119.

Sih, G.C., 1974. Strain-energy-density factor applied to mixed mode crack problems. International Journal of Fracture 10: 305–321.

Lazzarin, P., Zambardi, R., 2001. A finite-volume-energy based approach to predict the static and fatigue behavior of components with sharp V-shaped notches. International Journal of Fracture 112 (3): 275-298.

De Monte, M., Quaresimin, M., Lazzarin, P., 2007. Modelling of fatigue strength data for a short fibre reinforced polyamide 6.6 based on local strain energy density. 16th international conference on composite materials. Kyoto.

Ibáñez-Gutiérrez, F.T., Cicero, S., Madrazo, V., Berto, F., 2018. Fracture Loads Prediction on Notched Short Glass Fibre reinforced Polyamide 6 Using the Strain Energy Density. Physical Mesomechanics 21 (2): 165-172.

Sánchez, M., Cicero, S., Torabi, A.R., Ayatollahi, M.R., 2021. Critical Load Prediction in Notched E/Glass–Epoxy-Laminated Composites Using the Virtual Isotropic Material Concept Combined with the Average Strain Energy Density Criterion. Polymers 13 (7): 1057.
Bernasconi, A., Davoli, P., Basile, A., Filippi, A., 2007. Effect of fibre orientation on the fatigue behaviour of a short glass fibre reinforced polyamide-6. International Journal of Fatigue 29: 199–208.
Hansen, A.C., Garnich, M.R., 1995. A multicontinuum theory for structural analysis of composite materials systems. Composites Engineering 5 (9): 1091-1103.